A Multivector Variable Area Type Capacitive Angular Displacement Encoder Based on a Rotating Electric Field and Improvement of Its Demodulation Method

Xu Gao and Xuebin Zhang

***Abstract*—The problems of the traditional type grating angular displacement encoder make it difficult to balance the measurement performance of miniaturization, high precision and high resolution, and the ability to resist vibration and shock is poor. In this article, a multivector variable-area capacitive angular displacement encoder based on a rotating electric field is proposed. Based on the principle of constructing a rotating electric field, a three-layer transmissive sensing structure with upper and lower layers of electrode plates and a modulation rotor as the middle layer is proposed and designed. A single-channel signal is used as the input excitation signal of the capacitive sensor to avoid the problem of mismatching multiple input signals. A pair of quadrature signals reflecting the spatial angle information is obtained through electric field demodulation and differential processing. The phase demodulation method based on the time scale is further adopted to improve the precision of demodulation. Simulations and experiments show that the sensor has a diameter of 50 mm, a thickness of 5 mm, a resolution of 0.81″, an accuracy of 2.5″, and a maximum nonlinear error of 40″. The design is verified to be feasible, which provides a new solution for capacitive angular position sensor design.**

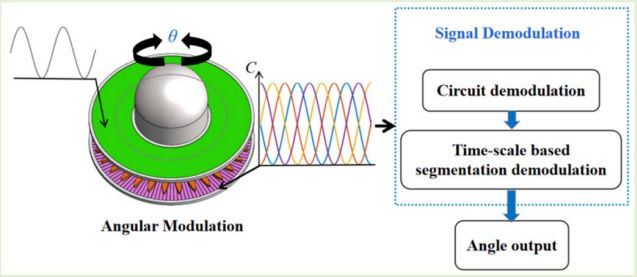

***Index Terms*— Angle measurement, capacitive sensing, rotating electric field, time scale demodulation.**

I. Introduction

THE development of aerospace and other industrial fields has led to increasing requirements for the measurement performance of rotary angular displacement encoders. Encoders are required to have high accuracy and high resolution; in addition, higher requirements are also needed in terms of their resistance to interference, vibration, and shock, as well as their size. In summary, the field of rotary angular displacement encoder measurement is moving toward high accuracy, high performance, and miniaturization [1].

Currently, most of the common angular displacement sensors are grating angular displacement encoders [1], which use diffraction gratings as the core components and the grating pitch as a reference to achieve angular displacement measurement. The German Heidenhain Company and the British Renishaw Company are the research and development sources for typical grating sensors. Heidenhain's highest bit absolute encoders are with a resolution of up to 31 bits [2]. The 24-bit absolute optical encoder designed by Changchun Institute of Optics, Fine Mechanics and Physics of China, has a resolution of 0.077″ and an accuracy of 0.51″ [3]. To miniaturize the encoder and improve its vibration and shock resistance, researchers have improved the encoder design by encoding-scheme improvements [4], image demodulation [5], [6], [7], [8], and fabrication of metal code disks [9] to improve the measurement performance and environmental adaptability of the encoder, but there are still some limitations.

Researchers found that the capacitive angular displacement encoder has not only a simple structure and small size, but also a faster response speed and better antivibration and shock ability compared with the grating angular displacement encoder.

Manuscript received 14 July 2022; revised 13 August 2022; accepted 17 August 2022. Date of publication 25 August 2022; date of current version 30 September 2022. This work was supported in part by the State Key Laboratory of Applied Optics under Grant SKLAO2021001A03, in part by the Key Research and Development of Jilin Provincial Department of Science and Technology-Key Industrial Core Technology Research Project under Grant 20210201091GX, and in part by the National Natural Science Foundation of China under Grant 62005101. The associate editor coordinating the review of this article and approving it for publication was Dr. Sanket Goel. *(Corresponding author: Xu Gao.)*

Xu Gao is with the School of Opto-Electronic Engineering and the State Key Laboratory of Applied Optics, Changchun University of Science and Technology, Changchun 130022, China (e-mail: gaox19870513@163.com).

Xuebin Zhang is with the School of Photoelectric Engineering, Changchun University of Science and Technology, Changchun 130022, China (e-mail: 2546751953@qq.com).

Digital Object Identifier 10.1109/JSEN.2022.3200099

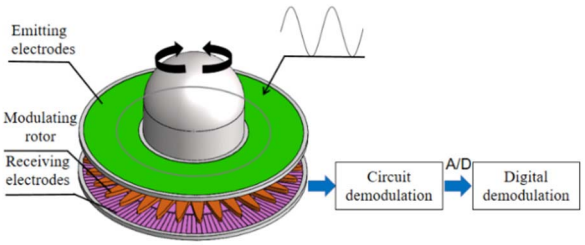

Fig. 1. Structural schematic of the capacitive angular position sensor based on a rotating electric field.

Its research value has been widely recognized. Starting in 1998, the team of Brasseur and others studied capacitive angular displacement encoders and proposed several solutions and improvements [10], [11], [12].

In recent years, the Israeli company Netzer [13], [14], [15], [16] developed the DS series encoder with the following dimensions: 58-mm diameter, 12.7-mm inner diameter, and 17-mm thickness, which is capable of achieving 18–20 bit resolution. The Hubei University of Technology, China [17], designed a multisignal input capacitive encoder achieving a resolution of 108″. Beijing University of Aeronautics and Astronautics [18] proposed the design of a two-layer structure capacitive encoder with an accuracy of 21.6″ and a resolution of 7.2″. Tsinghua University [19] improved the modulation of the signal to achieve a measurement accuracy of 12.96″ and a resolution of 3.24″. Changchun University of Science and Technology [20] designed a three-layer structure capacitive encoder with an accuracy of 21.6″.

The angular displacement encoder produced by Netzer Company uses four-way square waves with a phase shift of 90° as the input signal. This multiexcitation method has high requirements on the matching degree of the input signal and is prone to unbalanced errors. Moreover, most of the methods in the above literature used amplitude demodulation methods. Amplitude demodulation's robustness and accuracy are lower than those of phase demodulation methods. Therefore, in this article, a variable-area capacitive angular position sensor with a three-layer sensing structure is proposed and designed, which uses the phase demodulation method based on the time scale. This scheme was proposed with a single excitation and multiple outputs, avoiding the matching degree problem of multiexcitation input, which improved the accuracy and robustness of the demodulation.

As shown in Fig. 1, based on the principle of constructing a rotating electric field, the sensor is designed with a three-layer structure of two coupling electrodes and a modulating rotor. Multiple groups of parallel capacitors are formed by the coupling of the emitter and the receiver. The modulating rotor is made into a sinusoidal model as a medium to modulate the angle information into periodic capacitance changes and further divides the whole circle of capacitors into four groups of 0°, 90°, 180°, and 270° at equal intervals. The dimensions of its final designed encoder are 50 mm in diameter and 5 mm in thickness, which can obtain a resolution of 0.81″ and an accuracy of 2.5″.

This further lays the research foundation for the development of the new capacitive angular position sensor, which has a certain practical value.

II. Measurement Principle

A. Design of a Three-Layer Transmissive Sensing Structure Based on a Rotating Electric Field

Min *et al.* [21] proposed a method for angle measurement, where a rotating light field was constructed to obtain two columns of time–space orthogonal standing wave signals, and then two columns of standing wave signals were synthesized to generate traveling wave signals. The rotating electric field is constructed by following the principle of the rotating optical field. In contrast, the basic structure and preparation process of the rotating electric field is relatively simple and easy to achieve.

The construction of a spatially and temporally periodic rotating electric field requires spatial and temporal modulations of the electric field. To construct a uniformly varying rotating electric field, a sensing structure, as shown in Fig. 2, is designed. It consists of three parts: the emitter, the modulating rotor, and the receiver [shown as ①, ②, and ③ in Fig. 2, respectively]. Its structural characteristics are as follows.

1) *Emitter ①:* The emitter consists of a complete circle of electrodes and is connected to the input signal $V = V_0 (\cos(\omega t))$. The process by which the emitter supplies an input signal of frequency ω to the electric field achieves time modulation.
2) *Receiver ③:* The receiver consists of multiple electrodes arranged in a ring parallel to the emitter to form multiple groups of parallel coupling capacitors. Its electrical connection is shown in Fig. 2 ④. Four electrodes are adjacent for a cycle, arranged in a cycle of the same position as the connected electrodes.
3) *Modulation Rotor ②:* This rotor is used as the medium for multiple groups of parallel coupling capacitors composed of emitters and receivers. Its model is a ring-shaped sine curve. The polar coordinate equation is $r(\theta) = R + A\sin(N \times \theta)$. R is the radius of the model circle. A is the amplitude of the sine curve. N is the number of periods of the rotor, which is the same as the number of periods of the receiver. The structure in which the modulating rotor faces the receiving pole is shown in Fig. 2 ④. As the modulating rotor rotates by δ, the area of each receiver facing the modulating rotor varies periodically, and thus the capacitance changes periodically with the change in angle. This process is spatial modulation.

As shown in Fig. 2 ④, the whole circle of capacitors is divided into four groups of 0°, 90°, 180°, and 270° at equal intervals. One cycle of the four groups of capacitors corresponds to one cycle of the modulating rotor. As shown in Fig. 2 ②, one cycle of the modulating rotor corresponds to the spatial angle θ. When the modulating rotor turns θ, the four groups of capacitors change by one cycle. The modulating rotor has a total of N cycles, where $N = 2^n$ and $\theta = 360°/N$. The resolving power that the sensor can

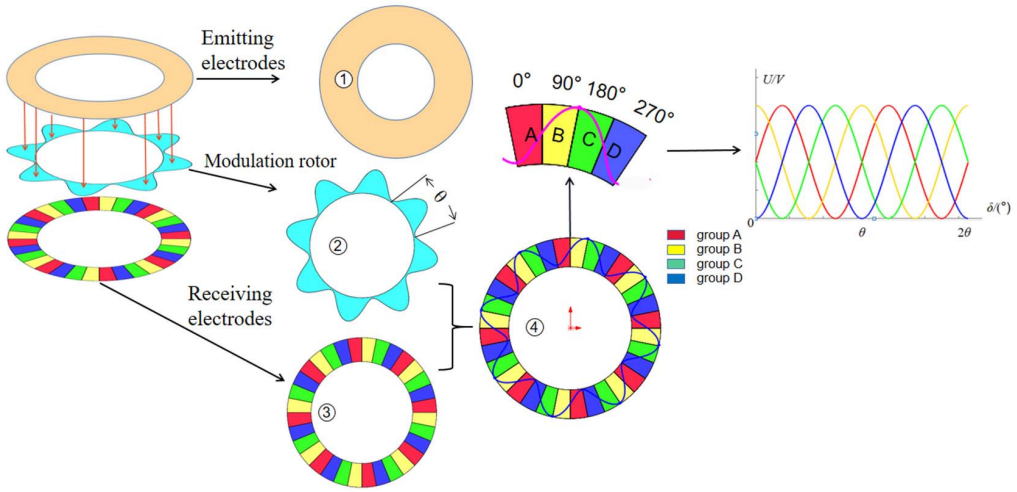

Fig. 2. Construction principle of the rotating electric field.

achieve before subdivision depends on the value of N. Its hardware resolving power can reach n bits with a minimum resolving angle of θ. A single cosine signal is used as the input excitation signal for the capacitive sensor to achieve temporal modulation while modulating the rotor rotation to achieve spatial modulation. The four output signals are demodulated and differentially processed to obtain a pair of quadrature signals reflecting the spatial angle information.

B. Sensor Sensing System Measurement Signal Analysis

Multiple parallel coupling capacitors are formed by the emitter and the receiver. The medium of each coupling capacitor consists of a modulating rotor with a fixed dielectric constant and air. Its specific expression is as follows:

$$C = \frac{\varepsilon_0 S}{d} + \frac{\varepsilon - \varepsilon_0}{d} \times s_1 \tag{1}$$

where ε_0 is the dielectric constant of the air, ε is the dielectric constant of the rotor, S is the area of one electrode, and S_1 is the area of the electrode facing the rotor. When the modulating rotor rotates, the modulating rotor plays the role of modulating the capacitance change. The area of the four groups of coupling capacitors in one period facing the modulating rotor is calculated as follows:

$$\begin{cases} S(\delta)_{0^\circ} = \displaystyle\int_{0+\delta}^{\alpha+\delta} \frac{1}{2} \times [R + A\sin(N \times \theta)]^2 \, d\theta \\ \qquad \times -\frac{1}{2} \times \theta \times R^2 \\ S(\delta)_{90^\circ} = \displaystyle\int_{\alpha+\delta}^{2\alpha+\delta} \frac{1}{2} \times [R + A\sin(N \times \theta)]^2 \, d\theta \\ \qquad \times -\frac{1}{2} \times \theta \times R^2 \\ S(\delta)_{180^\circ} = \displaystyle\int_{2\alpha+\delta}^{3\alpha+\delta} \frac{1}{2} \times [R + A\sin(N \times \theta)]^2 \, d\theta \\ \qquad \times -\frac{1}{2} \times \theta \times R^2 \\ S(\delta)_{270^\circ} = \displaystyle\int_{3\alpha+\delta}^{4\alpha+\delta} \frac{1}{2} \times [R + A\sin(N \times \theta)]^2 \, d\theta \\ \qquad \times -\frac{1}{2} \times \theta \times R^2 \end{cases} \tag{2}$$

where α is the central angle corresponding to an electrode and δ is the angle through which the modulating rotor is turned. After calculation, the area change equation of the four groups of coupling capacitors facing the modulation rotor is as follows:

$$\begin{cases} S(\delta)_{0^\circ} = B + B\sin(n\delta) \\ S(\delta)_{90^\circ} = B + B\cos(n\delta) \\ S(\delta)_{180^\circ} = B - B\sin(n\delta) \\ S(\delta)_{270^\circ} = B - B\cos(n\delta). \end{cases} \tag{3}$$

B is 1/2 of the maximum value of the area of one coupling capacitor facing the modulated rotor. The area change curves of four coupling capacitors facing the modulated rotor differ in phase by $\pi/2$. By substituting the area change into the capacitance calculation formula, four coupling capacitance change formulas within a cycle can be obtained

$$\begin{cases} C_{0^\circ} = \dfrac{\varepsilon_0 S}{d} + \dfrac{\varepsilon - \varepsilon_0}{d} \times [B + B\sin(n\delta)] \\ C_{90^\circ} = \dfrac{\varepsilon_0 S}{d} + \dfrac{\varepsilon - \varepsilon_0}{d} \times [B + B\cos(n\delta)] \\ C_{180^\circ} = \dfrac{\varepsilon_0 S}{d} + \dfrac{\varepsilon - \varepsilon_0}{d} \times [B - B\sin(n\delta)] \\ C_{270^\circ} = \dfrac{\varepsilon_0 S}{d} + \dfrac{\varepsilon - \varepsilon_0}{d} \times [B - B\cos(n\delta)]. \end{cases} \tag{4}$$

The above analysis shows the modulation changes of the four groups of capacitors after the modulating rotor pairs split phase in space. After the input signal is applied, the space/time modulation is realized simultaneously, and a rotating voltage signal with the voltage varying with the angle is obtained. The input signal is applied to the emitter, and the four output signals U_{0°, U_{90°, U_{180°, and U_{270° are obtained after C–V conversion

$$\begin{cases} U_{0^\circ} = K[\cos(\omega t) + \cos(\omega t)\sin(n\delta)] \\ U_{90^\circ} = K[\cos(\omega t) + \cos(\omega t)\cos(n\delta)] \\ U_{180^\circ} = K[\cos(\omega t) - \cos(\omega t)\sin(n\delta)] \\ U_{270^\circ} = K[\cos(\omega t) - \cos(\omega t)\cos(n\delta)]. \end{cases} \tag{5}$$

Difference U_{0° from U_{180° and U_{90° from U_{270° to obtain a pair of orthogonal signals responding to the

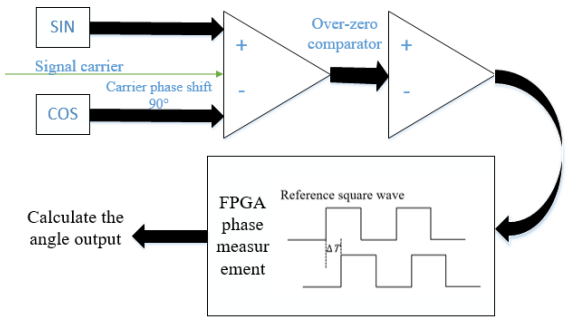

Fig. 3. Demodulation diagram.

angular information

$$\begin{cases} U_{0^\circ} - U_{180^\circ} = 2K\left[\cos\left(\omega t\right)\sin\left(n\delta\right)\right] \\ U_{90^\circ} - U_{270^\circ} = 2K\left[\cos\left(\omega t\right)\cos\left(n\delta\right)\right]. \end{cases} \tag{6}$$

A pair of quadrature amplitude modulation signals reflecting the spatial angle information is obtained. Subsequently, the solution phase can be subdivided and calculated by synthesizing traveling wave signals.

C. Time-Scale-Based Signal Demodulation Implementation

The output signal is shown in (6). The output signal is similar in form to the output signal of the resolver. Generally, a dedicated demodulation chip is used for demodulation, such as an AD2S1210. However, the amplitude demodulation has the problem of low demodulation accuracy and poor robustness. The two signals are further processed, the phase of one signal is shifted by 90°, and then the difference is made with the other signal to obtain a traveling wave signal. The angular displacement information is reflected in the phase of the output signal, which avoids the demodulation error caused by the disturbance of the amplitude demodulation, and further improves the robustness of the system

$$\begin{aligned} &\left(U_{0^\circ} - U_{180^\circ}\right) - \left(U_{90^\circ} - U_{270^\circ}\right)' \\ &\quad = 2K\left[\cos\left(\omega t\right)\sin\left(n\delta\right) + \sin\left(\omega t\right)\cos\left(n\delta\right)\right] \\ &\quad = 2K\sin\left(\omega t + n\delta\right). \end{aligned} \tag{7}$$

When the modulating rotor rotates through an angle, the output signal produces a phase change corresponding to the angle. As shown in Fig. 3, the output signal is shaped into a square wave signal by an over-zero comparator, and the FPGA chip is used to achieve the angle measurement by comparing the phase with the reference square wave signal and always using high-frequency pulses to achieve phase interpolation.

III. Principle Simulation Analysis

A 3-D electric field finite-element simulation of the designed sensing structure based on a rotating electric field was carried out to verify the modulation of the four sets of capacitors by the modulating rotor in space and calculate specific results. First, for the overall model design, the modulated rotor is designed for 32 cycles, with one cycle corresponding to a spatial angle of 11.25°. The rotor model design is shown in Fig. 4(a); the corresponding emitter and receiver poles are shown in Fig. 4(b) and (c), respectively.

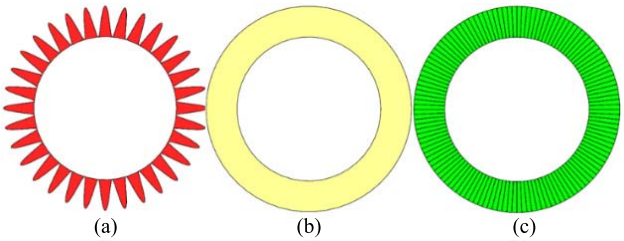

Fig. 4. Design of the simulation model. (a) Modulation Rotor. (b) Emitter. (c) Receiver.

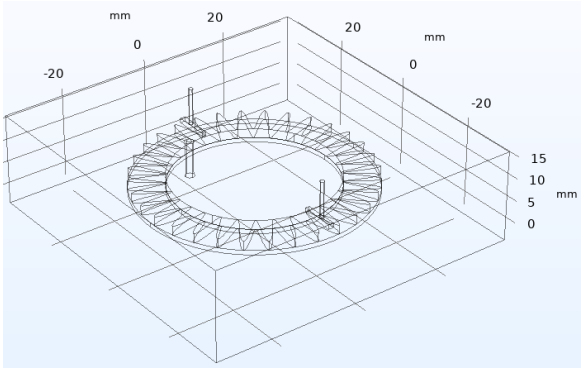

Fig. 5. 3-D view of the simulation model.

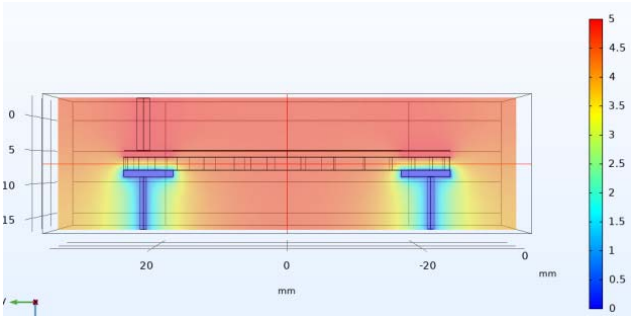

Fig. 6. Results of electric field simulation.

The 3-D view is shown in Fig. 5, with a model radius of 50 mm, an inner diameter of 35 mm, and a thickness of 5 mm (rotor: 2 mm; emitter and receiver: 1 mm; gap on both sides: 0.5 mm). The modulating rotor has an invariant and uniformly distributed dielectric constant, the entire model is in an air environment, the emitter is supplied with 5 V, and the receiver is grounded. A simulation of the electric field in space for one of the angles at which the rotor is located is shown in Fig. 6. By calculating its Maxwell capacitance value, the exact value of the rotor's four capacitances at this angle can be obtained.

Resimulate and calculate capacitance after every 1.125° rotation of the modulating rotor, and the variation of the four sets of coupling capacitances at 0°, 90°, 180°, and 270° during the dynamic rotation of the modulated rotor can be obtained. The calculated data are shown in Table I, and the data curves are shown in Fig. 7.

TABLE I
SIMULATED CAPACITANCE DATA

Angle/°	0°Phase/F	90°Phase/F	180°Phase/F	270°Phase/F
0°	1.60624E-11	1.47488E-11	1.32074E-11	1.47635E-11
1.125°	1.58189E-11	1.39422E-11	1.3547E-11	1.554E-11
2.25°	1.51571E-11	1.32894E-11	1.4341E-11	1.59902E-11
3.375°	1.43448E-11	1.33016E-11	1.51621E-11	1.59608E-11
4.5°	1.35528E-11	1.39496E-11	1.58483E-11	1.55485E-11
5.625°	1.32072E-11	1.47635E-11	1.6056E-11	1.47461E-11
6.75°	1.3547E-11	1.554E-11	1.58266E-11	1.39331E-11
7.875°	1.4341E-11	1.59901E-11	1.51482E-11	1.32982E-11
9°	1.51621E-11	1.59608E-11	1.43362E-11	1.32997E-11
10.125°	1.58483E-11	1.55485E-11	1.35501E-11	1.39576E-11
11.25°	1.6056E-11	1.47461E-11	1.32038E-11	1.47371E-11

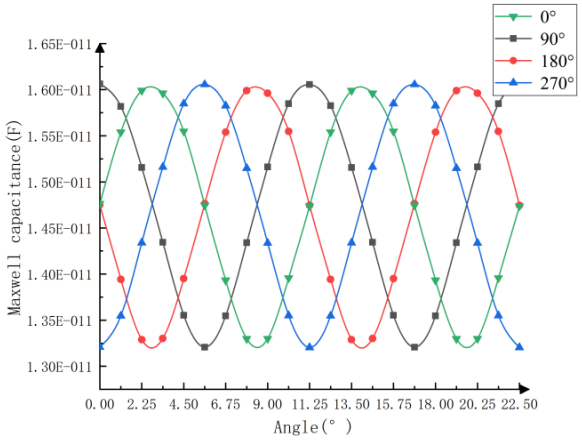

Fig. 7. Capacitance change curve of simulation results.

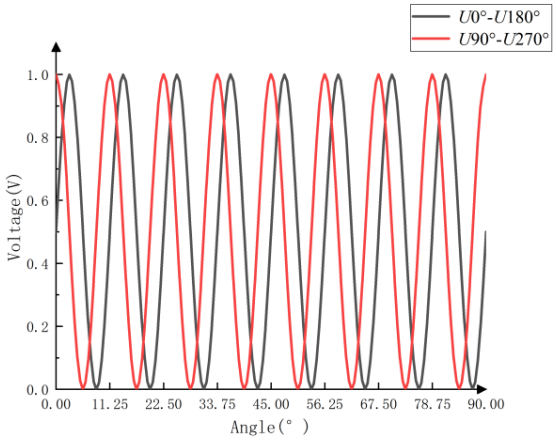

Fig. 8. Simulate the signal output result of the demodulation circuit.

The four groups of capacitors in one cycle exhibit sinusoidal periodic changes, and the phase difference of the capacitance change curves of adjacent phases is 90°. Therefore, modulating the rotor can cause the modulation of four groups of capacitors in space. Using the obtained capacitance change data as a model, the input signal is applied as a 5 V, 1 kHz cosine excitation signal. The circuit for the simulation is built based on the above theory. The output four signals are demodulated by the circuit to obtain two quadrature amplitude modulation signals with the angle change, and the corresponding amplitude value of each angle is recorded as shown in Fig. 8.

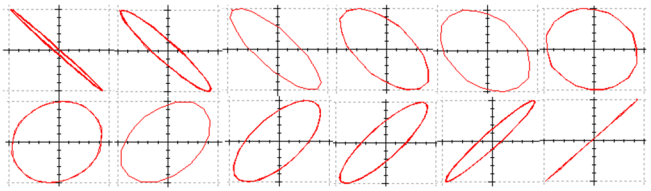

Fig. 9. Lissajous-figure simulation results are shown.

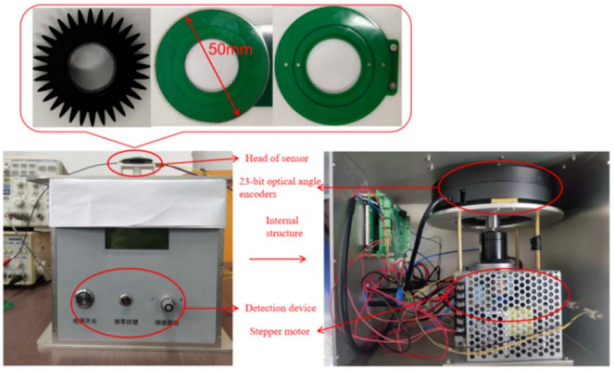

Fig. 10. Sensing structure and detection device.

Using the demodulation method based on the time scale, a simulation circuit is built to obtain the output signal and compare it with the reference signal. Fig. 9 shows the phase comparison results of the output signal and the reference signal using capacitance simulation data from 0° to 5.625°. The diagram shows the half-cycle phase change, and the phase change rule is as follows.

When the capacitors of the 0° phase and 180° phase are at the maximum capacitance difference and the capacitors of the 90° phase and 270° phase have equal capacitance, the phase difference is 0 or π. In contrast, the phase difference is $\pi/2$ or $3\pi/2$ when the capacitors of the 90° phase and 270° phase are at the maximum capacitance difference and the capacitors of the 0° phase and 180° phase have equal capacitance.

The simulation verifies the feasibility of the above theory from field analysis to demodulation circuit.

IV. EXPERIMENTS

A. Sensor System Prototype Construction and Calibration Test

Based on the above theoretical and simulation analysis, the experimental platform was built as shown in Fig. 10. The parameters of the prototype are consistent with the simulation design, and the emitter and receiver poles are made by standard PCB processing. The 23-bit photoelectric shaft angle encoder is used to perform relative calibration (the resolution of the 23-bit photoelectric shaft angle encoder is 0.154″, and the accuracy is better than 0.3″).

B. Implementation of Prototype Signal Processing

A 1-kHz, 5-V input signal is provided. Modulation rotor rotation is controlled by the motor. The demodulation block diagram is shown in Fig. 11. The prototype outputs four

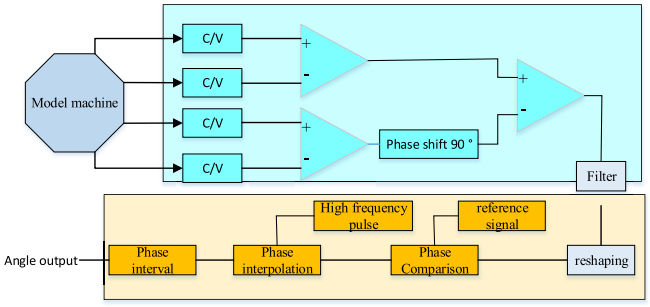

Fig. 11. Overall demodulation block diagram.

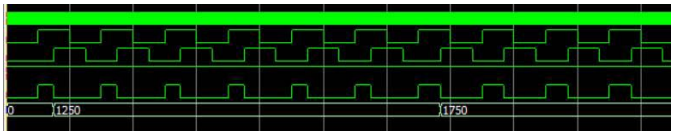

Fig. 12. FPGA timing chart.

signals, and through the analog circuit demodulation module, outputs a pair of orthogonal signals. The quadrature amplitude modulation signal is processed by using (7) to obtain an electric traveling wave signal with phase varying with angle. After the traveling wave signal is converted into a square wave signal, phase comparison is performed with the reference signal. The time of the phase difference is obtained by high-frequency pulse interpolation, and the angle information is calculated and output with the upper computer.

In the analog circuit, the C–V conversion is performed by the 4-channel current amplifier circuit. Following the above theory, the corresponding phase signals are differenced and then output a pair of quadrature amplitude modulation signals. After the difference, the signal frequency is 1 kHz, so the quality of the output signal can be improved by using a bandpass filter of the corresponding frequency. Finally, it is converted into a square wave signal for processing through a zero-crossing comparator.

The digital circuit processing part is based on FPGA as the core device; here, the EP4CE6F17 type chip made by ALTERA is used. The design is as follows.

A 50-MHz crystal is used, and two counters are designed to realize the generation of the reference square wave and the interpolation of the phase difference, with the timing shown in Fig. 12.

C. Signal Output Results of the Prototype

Based on the above experimental scheme design, the output signal is obtained by building the experiment, and the following data are the results obtained by using a data acquisition card (usb3133A type produced by Beijing ART, acquisition rate 500 kps/s, resolution 16 bit). The results of the reference signal and output are shown in Fig. 13(a). The output signal is characterized by the same frequency as the reference signal, and the phase differs from the reference signal by ΔT. Three sets of dynamic output signals shown in (6) are also collected.

Fig. 13(b) shows the output signal results of three different speeds. The fundamental frequency of the output signal is 1 kHz, and the amplitude of the fundamental wave of the

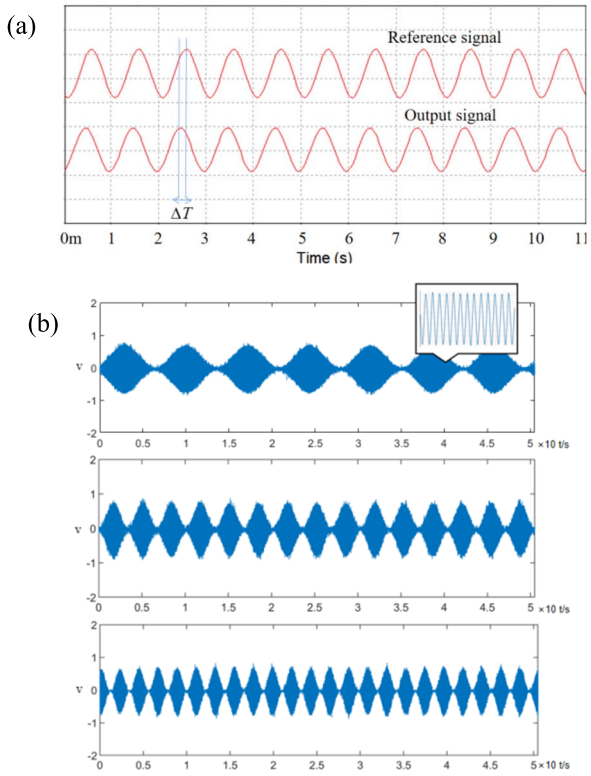

Fig. 13. (a) Reference signal and output signal. (b) Output waveforms acquired at three different speeds.

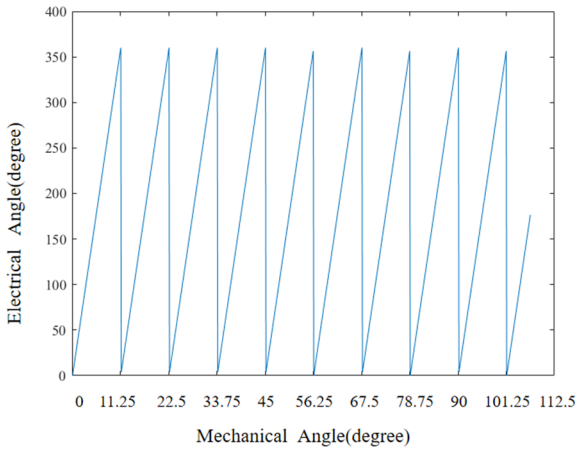

Fig. 14. Angle data output results.

output signal changes with the sine–cosine law as the angle rotates. The results of the signal output show the correctness of the above theory. However, with external interference, the amplitude information will be disturbed, and the output signal amplitude variation law cannot present the ideal state of the sine cosine. Fig. 14 shows the angle data of the motor output at a speed of 10°/s.

V. Prototype Performance Testing

A. Accuracy Test

Using the above device, a preliminary accuracy test of the sensor's sensing structure was conducted. When the rotor is at

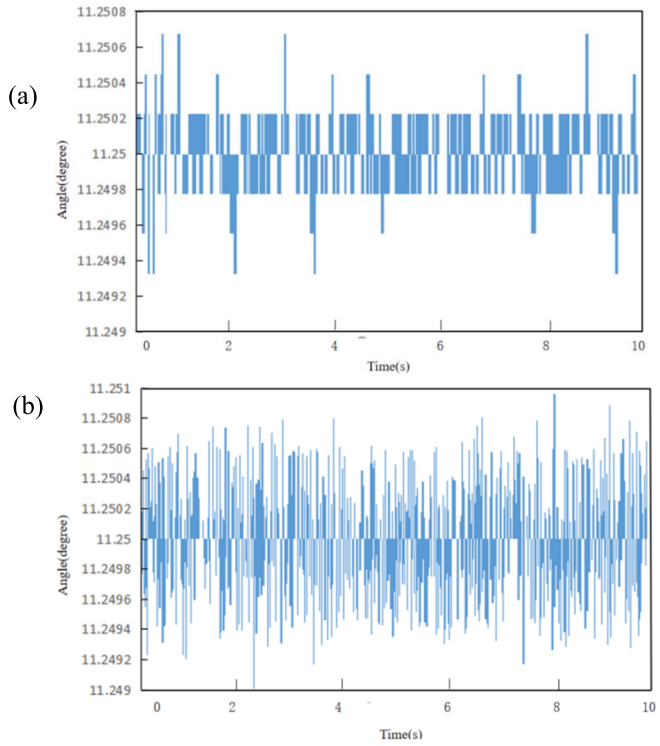

Fig. 15. Measurement error curve. (a) Demodulation method in this article. (b) Amplitude demodulation method.

rest, the output angle is shown in Fig. 15(a). The test shows that the accuracy is <2.5″ and its minimum resolution is 0.81″.

At the same time, the acquisition card was used to collect quadrature amplitude voltage amplitude information. The calculated angle information is shown in Fig. 15(b). The output angle accuracy is <3.6″. Therefore, the correctness and accuracy of the phase demodulation method based on the time scale are better than those of the amplitude demodulation method.

B. Nonlinearity

The dynamic nonlinearity of the prototype was analyzed by comparing the high shaft angle encoder output angle as a reference with the prototype measurement data. The results are shown in Fig. 16(a), and Fig. 16(b) shows the nonlinear error, where the maximum nonlinear error is 40″.

The main factors affecting the nonlinearity of the prototype are the following: errors caused by mounting and processing errors, errors caused by vibration shock of the shaft system, unbalance of capacitance caused by deviation of the electrode shape from the ideal shape when the PCB is made, and electromagnetic interference caused by the absence of housing shielding.

The size and resolution of commercial angular displacement encoders are listed and compared with those proposed in this article.

The data in Table II shows that under the similar resolution condition, the angular displacement encoder proposed in this article has a smaller volume, especially in thickness

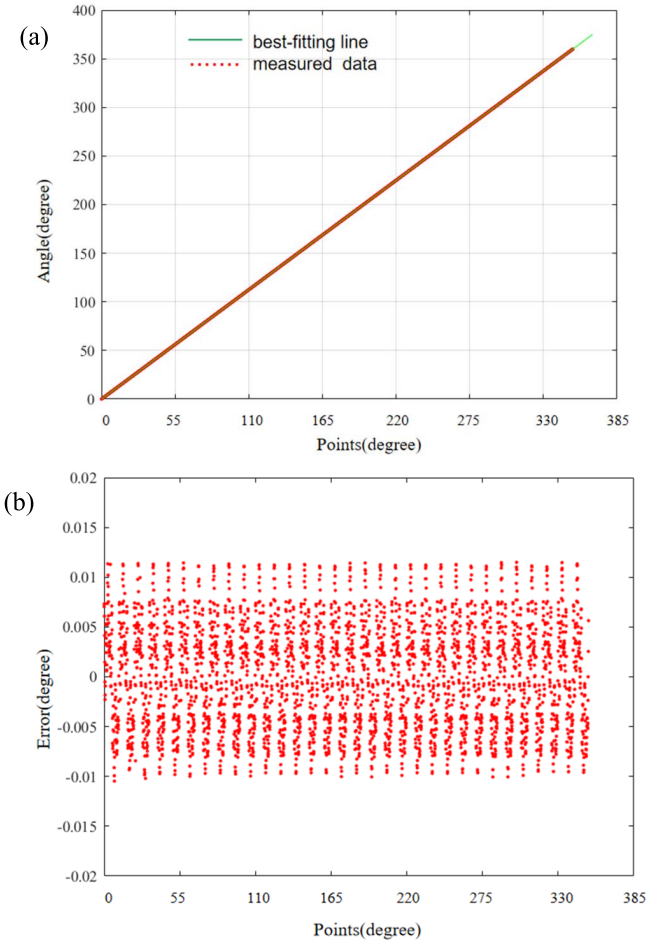

Fig. 16. (a) Measurement results and best-fit curves. (b) Nonlinear error diagram.

TABLE II
COMMON ENCODER PARAMETERS

Model of angular displacement encoder	Size	resolution
(Heidenhain)ECI1319	Diameter:56 mm、Thickness:32 mm	2.47″(19bit)
(Tamagawa)SA48	Diameter:100 mm、Thickness:51 mm	9.88″(17bit)
GEX58011K1R4096	Diameter:60 mm、Thickness:40 mm	19.77″(16bit)
GES58011K1R4096	Diameter:60 mm、Thickness:40 mm	19.77″(16bit)
The scheme of this paper	Diameter:50 mm、Thickness:5 mm	0.81″(20-21bit)

parameters. Therefore, the scheme proposed in this article has better application prospects.

VI. CONCLUSION

A multivector variable-area type capacitive angular position sensor based on a rotating electric field is proposed, drawing on the principle of rotating light field generation. A three-layer

transmissive sensing structure with upper and lower electrode plates and modulating rotor as the middle layer is proposed and designed using a ring-shaped sinusoidal modulating rotor. The whole circle of the capacitive split phase is divided into four groups of 0°, 90°, 180°, and 270° at equal intervals. A single signal is used as an input signal for the encoder, and a pair of orthogonal signals reflecting spatial angle information is obtained through circuit demodulation and differential processing. The demodulation method based on the time scale is used to achieve demodulation. This scheme can effectively reduce the size of the angular displacement sensor, improve its ability to resist vibration and shock, and improve the accuracy and robustness of demodulation.

The finite-element analysis of the proposed three-layer measurement structure verifies rotor-to-capacitance modulation variation and obtains the original capacitance change data, and the angle measurement can be obtained after the simulation circuit demodulation. The experimental results show that the designed sensor structure has a diameter of 50 mm, a thickness of 5 mm, a resolution of 0.8″, an accuracy of 2.4″, and a maximum nonlinear error of 40″, which provides a new scheme for capacitive angular position sensors. The research results lay the theoretical foundation for further demodulation and have certain practical value.

REFERENCES

[1] L. Li, "Displacement measuring technology based on diffractive light of grating interference," Graduate School Chin. Acad. Sci., Changchun Inst. Opt., Precis. Mach. Phys., 2010. [Online]. Available: https://kns.cnki.net/KCMS/detail/detail.aspx?dbname=CDFD0911&filename=2010180765.nh

[2] C.-F. Kao, H.-L. Huang, and S.-H. Lu, "Optical encoder based on fractional-Talbot effect using two-dimensional phase grating," *Opt. Commun.*, vol. 283, no. 9, pp. 1950–1955, May 2010.

[3] X. Jingwu and W. Qiuhua, "23-bit photoelectric rotary encoder," *Opt. Mach.*, vol. 113, no. 2, pp. 52–60, 1990.

[4] W. Yuanyuan, "Research on key technologies of small single turn absolute photoelectric encoder," Graduate School Chin. Acad. Sci., Changchun Inst. Opt., Precis. Mach. Phys., 2012. [Online]. Available: https://kns.cnki.net/KCMS/detail/detail.aspx?dbname=CMFD201401&filename=1013282015.nh

[5] D. B. Leviton and B. Frey, "Ultrahigh-resolution absolute position sensors for cryostatic applications," *Proc. SPIE*, vol. 4850, pp. 776–787, Mar. 2003.

[6] D. Leviton and M. S. Garza, "Recent advances and applications of NASA's new ultrahigh-sensitivity absolute optical pattern recognition encoders," *Proc. SPIE*, vol. 4091, pp. 375–384, Oct. 2000.

[7] Y.-N. Wang, B. Yaun, and X.-X. Ni, "Subdivision technique of absolute angular encoder using array detector," *J. Zhejiang Univ., Eng. Sci.*, vol. 45, pp. 370–374, Feb. 2011.

[8] C. Yun, "Research on the principle of single turn absolute photoelectric shaft angle encoder," Graduate School Chin. Acad. Sci., Changchun Inst. Opt., Precis. Mach. Phys., 2006. [Online]. Available: https://kns.cnki.net/KCMS/detail/detail.aspx?dbname=CDFD9908&filename=2006179499.nh

[9] W. Yubing *et al.*, "Small high-resolution metal encoder," Ph.D. dissertation, Adv. Laser Optoelectron., 2019, vol. 56, no. 18.

[10] G. Brasseur, "A capacitive finger-type angular-position and angular speed sensor," *IEEE Instrum. Meas.*, vol. 18, no. 20, pp. 967–972, May 1998.

[11] M. Gasulla, X. Li, G. C. M. Meijer, L. van der Ham, and J. W. Spronck, "A contactless capacitive angular-position sensor," *IEEE Sensors J.*, vol. 3, no. 5, pp. 607–614, Oct. 2003.

[12] V. Ferrari, A. Ghisla, D. Marioli, and A. Taroni, "Capacitive angular-position sensor with electrically floating conductive rotor and measurement redundancy," *IEEE Trans. Instrum. Meas.*, vol. 55, no. 2, pp. 514–520, Apr. 2006.

[13] Y. Netzer, "Capacitive displacement encoder," U.S. Patent 6 492 911, Dec. 10, 2002.

[14] *Application Note 01—The Electric Encoder*, Netzer Precis. Motion Sensors Ltd., Misgav Ind. Park, Misgav, Israel, 2009.

[15] *Application Note 02—Electrically Interfacing DS Electric Encoders*, Netzer Precis. Motion Sensors Ltd., Misgav Ind. Park, Misgav, Israel, 2009.

[16] *Application Note 05—Accuracy, Resolution, and Repeatability*, Netzer Precis. Motion Sensors Ltd., Misgav Ind. Park, Misgav, Israel, 2008.

[17] H. Jun *et al.*, "Design and application of capacitive grating rotary encoder," *J. Hunan Univ. Technol.*, vol. 29, no. 5, pp. 45–50, 2015.

[18] D. Zheng, S. Zhang, S. Wang, C. Hu, and X. Zhao, "A capacitive rotary encoder based on quadrature modulation and demodulation," *IEEE Trans. Instrum. Meas.*, vol. 64, no. 1, pp. 143–153, Jan. 2015.

[19] B. Hou, B. Zhou, M. Song, Z. Lin, and R. Zhang, "A novel single-excitation capacitive angular position sensor design," *Sensors*, vol. 16, no. 8, p. 1196, Jul. 2016.

[20] X. Cui, "Research on capacitive absolute coded angular displacement sensors," Graduate School Changchun Univ. Sci. Technol., Sep. 2019. [Online]. Available: https://kns.cnki.net/KCMS/detail/detail.aspx?dbname=CMFD202001&filename=1020705840.nh

[21] F. Min *et al.*, "High-precision angular displacement measurement based on rotating optical field," *Acta Optica Sinica*, vol. 41, no. 18, pp. 1–10, 2021.

Xu Gao received the bachelor's degree from Jilin University (JLU), Changchun, China, in 2009, and the Ph.D. degree from the Changchun Institute of Optics, Fine Mechanics and Physics (CIOMP), Changchun, in 2014.

She is working with the School of Opto-Electronic Engineering, Changchun University of Science and Technology (CUST), Changchun. Her current research interests include photoelectric precise displacement measurement technology and photoelectric sensors.

Xuebin Zhang received the bachelor's degree from the Inner Mongolia University of Technology (IMUT), Hohhot, China, in 2020. He is currently pursuing the master's degree in instrumentation engineering with the Changchun University of Science and Technology (CUST), Changchun, China.

His main research interests lie in sensor signal processing.